

Performance Analysis of IEEE 802.11bn Non-Primary Channel Access

Boris Bellalta^b, Francesc Wilhelmi^b, Lorenzo Galati Giordano^{*}, and Giovanni Geraci^{‡b}

^b*Department of Engineering, Universitat Pompeu Fabra, Barcelona, Spain*

^{*}*Radio Systems Research, Nokia Bell Labs, Stuttgart, Germany*

[‡]*Nokia Standards, Spain*

Abstract—This paper presents a performance analysis of the Non-Primary Channel Access (NPCA) mechanism, a new feature introduced in IEEE 802.11bn to enhance spectrum utilization in Wi-Fi networks. NPCA enables devices to contend for and transmit on the secondary channel when the primary channel is occupied by transmissions from an Overlapping Basic Service Set (OBSS). We develop a Continuous-Time Markov Chain (CTMC) model that captures the interactions among OBSSs in dense WLAN environments when NPCA is enabled, incorporating new NPCA-specific states and transitions. In addition to the analytical insights offered by the model, we conduct numerical evaluations and simulations to quantify NPCA’s impact on throughput and channel access delay across various scenarios. Our results show that NPCA can significantly improve throughput and reduce access delays in favorable conditions for BSSs that support the mechanism. Moreover, NPCA helps mitigate the OBSS performance anomaly, where low-rate OBSS transmissions degrade network performance for all nearby devices. However, we also observe trade-offs: NPCA may increase contention on secondary channels, potentially reducing transmission opportunities for BSSs operating there.

Index Terms—Non-primary channel access, NPCA, IEEE 802.11bn, WLAN, Wi-Fi 8.

I. INTRODUCTION

The context: Wi-Fi channel widths have increased over time, from the initial 20 MHz to 320 MHz, going through 40, 80, and 160 MHz. The adoption of wider channels aims to enhance network performance by increasing transmission rates, improving throughput, and reducing latency. However, as a result of current channel sensing rules based on Listen Before Talk (LBT), this comes with the drawback of higher contention with neighboring networks operating on the same channel or overlapping portions of it [1].

Channels wider than 20 MHz consist of a mandatory 20 MHz primary channel—where all devices within the same Basic Service Set (BSS) perform channel access contention (e.g., backoff countdown)—and one or more secondary channels. Secondary channels can only be used if they are idle at the time a transmission opportunity is secured via the primary channel. If one or more secondary channels are occupied by an Overlapping BSS (OBSS), they are effectively bypassed by puncturing them thanks to the preamble puncturing feature introduced in IEEE 802.11ax (Wi-Fi 6) [2]. While this reduces the effective channel width, it still allows devices to transmit using the instantaneous available spectrum.

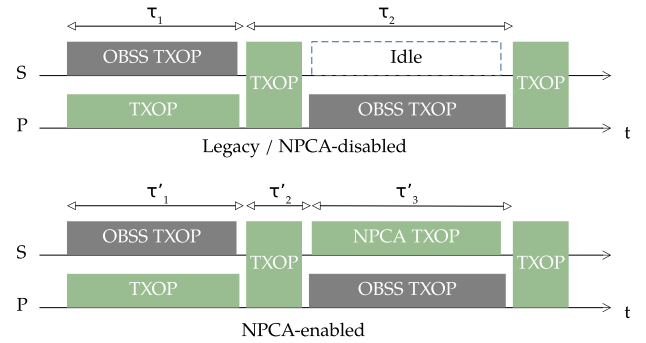


Fig. 1: Legacy vs. NPCA operation, where ‘P’ and ‘S’ denote the primary and secondary channel, respectively, e.g., an 80 MHz channel each. The figure illustrates how NPCA enables near-continuous transmissions, resulting in higher throughput and reduced channel access delays, as reflected by the lower times between consecutive channel accesses (τ values).

The problem: Wi-Fi currently lacks a solution for scenarios where the primary channel of a BSS is occupied by an OBSS transmission. In such cases, even if all the secondary channels are available, devices in the affected BSS must defer their transmissions until the primary channel becomes idle again. This results in reduced channel access opportunities and inefficient spectrum utilization, as illustrated in Fig. 1 (upper part).

The 802.11bn solution: To address this issue, IEEE 802.11bn [3], [4] is developing a new feature called Non-Primary Channel Access (NPCA). The concept is straightforward: when a BSS detects an OBSS transmission on its primary channel, NPCA-compliant devices switch to a secondary channel, designated as the NPCA primary channel, to perform channel contention and initiate transmissions while the primary is busy. This enables the BSS to utilize idle secondary channels effectively. The benefits of this approach are illustrated in Fig. 1 (lower part). With NPCA, the target BSS increases its chances of accessing the channel, which is crucial for latency-sensitive traffic, while ensuring the full utilization of available spectrum.

Our contribution: In this paper, we investigate the potential throughput and channel access delay gains of NPCA.

To achieve this, we use Continuous Time Markov Chains (CTMCs) to model the system behavior with and without NPCA. CTMCs have been widely and successfully applied to analyze the performance of complex Carrier Sense Multiple Access with Collision Avoidance (CSMA/CA) networks [5]–[7], including scenarios involving advanced features such as channel bonding [8]–[10] and spatial reuse [11]. Specifically, we extend CTMC modeling to capture NPCA operation, leveraging their suitability for studying CSMA/CA-based networks in general and Wi-Fi in particular.

The main contributions of this paper are as follows:

- 1) We extend CTMC 802.11 models to incorporate NPCA operation, enabling detailed performance analysis.
- 2) We evaluate NPCA numerically and demonstrate that it effectively provides throughput and channel access gains (up to $\times 2$ on average) for the NPCA-enabled BSS while remaining completely transparent to OBSS networks operating on the NPCA-enabled BSS primary channel.
- 3) We uncover the relationship between the Transmission Opportunity (TXOP) duration and NPCA performance, highlighting a trade-off between NPCA throughput gains and the Aggregated MAC Protocol Data Unit (A-MPDU) size.
- 4) We show that NPCA mitigates the OBSS performance anomaly, particularly when OBSS transmissions are disproportionately long due to using low Modulation and Coding Scheme (MCS), while the target BSS employs high MCSs. In such cases, throughput gains exceeding $\times 2$ can be achieved.
- 5) We illustrate that, in the presence of OBSSs operating on the secondary channel of the target NPCA BSS, enabling NPCA has a significant impact on the throughput distribution between the target BSS and the OBSSs.

II. NON PRIMARY CHANNEL ACCESS

The operation of NPCA is illustrated in Fig. 2, where the primary and secondary channels of a given BSS are shown. In the context of NPCA, we refer to the secondary channel as the *NPCA channel*. Additionally, the 20 MHz channel within the NPCA channel used for contention is referred to as the *NPCA primary channel*.

When an OBSS transmission is detected on an NPCA-enabled BSS's primary channel, after receiving both Request-To-Send (RTS) and Clear-To-Send (CTS) frames, all NPCA-capable devices switch their control channel to a predefined 20 MHz secondary channel (i.e., the NPCA primary channel). In this paper, we assume that contention on the NPCA primary channel begins after a delay of T_{NPCA} from the start of the OBSS transmission. This delay T_{NPCA} corresponds to the duration of the RTS/CTS exchange. Once the backoff counter reaches zero, a transmission on the secondary channel is initiated following the default 802.11 rules.

A key requirement of NPCA is that transmissions must complete before the OBSS transmission ends, so that the BSS can resume operation on its default primary channel. This constraint is important because not all devices within

the BSS are assumed to support NPCA. We also account for a switching delay, denoted T_{switch} , which represents the time required to return from the NPCA primary channel to the default primary channel. As a result, the time available for an NPCA transmission opportunity is limited by the duration of the OBSS transmission, reduced by the sum of T_{NPCA} and T_{switch} . These additional switching overheads reduce the effective time available for data transmission in NPCA, leading to slightly lower efficiency compared to legacy (non-NPCA) transmissions.

Finally, we make the following two assumptions regarding NPCA operation, both of which leverage the fact that the NPCA BSS is aware of the expected end time of the OBSS transmission occupying its primary channel:

- 1) After switching to the NPCA primary channel due to an OBSS transmission on the primary channel, if the NPCA primary channel is initially busy, the target BSS will continue to monitor it and attempt to transmit if it becomes idle before the NPCA opportunity ends.
- 2) If a transmission on the NPCA channel concludes and there is still sufficient time to initiate another transmission, the target BSS will re-contend for access on it by executing a new backoff procedure on the NPCA primary channel. If successful, it will initiate another transmission, with its duration adjusted to fit within the remaining time of the OBSS transmission.

In both cases, the target BSS returns to its default primary channel before the OBSS transmission completes.

III. SYSTEM MODEL

To analyze the NPCA performance, we consider the scenario depicted in Fig. 3. The scenario consists of four BSSs, each consisting of one AP and one STA. The channel allocation for each BSS is detailed in the figure: BSS A and C utilize 160 MHz channels, while BSS B and D operate on 80 MHz channels. All devices, including APs and STAs, are within each other's coverage area, eliminating the possibility of hidden terminals. For simplicity, the lower 80 MHz of the 160 MHz channel is referred to as channel 1 (Ch#1), and the upper 80 MHz as channel 2 (Ch#2). When APs A and C use the 160 MHz channel, it is indicated as utilizing both Ch#1 and Ch#2.

STAs are deployed at a distance d from their respective APs. The TMB path loss model for the 5 GHz band in indoor office environments is considered [12]. The selected MCS values depend on the received power and range from MCS 11 (1024-QAM; 5/6) to MCS 1 (BPSK; 1/2). The maximum TXOP duration is set to $T_{\text{max}} = 5$ ms, encompassing the RTS/CTS exchange, data transmission, Block Acknowledgment (BACK), and inter-frame spaces. A Packet Error Rate (PER) of 0.1 is assumed for all MCSs. All transmissions utilize two spatial streams for the data part, while one spatial stream is used for all control frames.

Only downlink traffic is considered, meaning that only Access Points (APs) transmit data packets. Throughout the paper, we use the terms AP and Basic Service Set (BSS) interchangeably to refer to the transmitting device. Each data

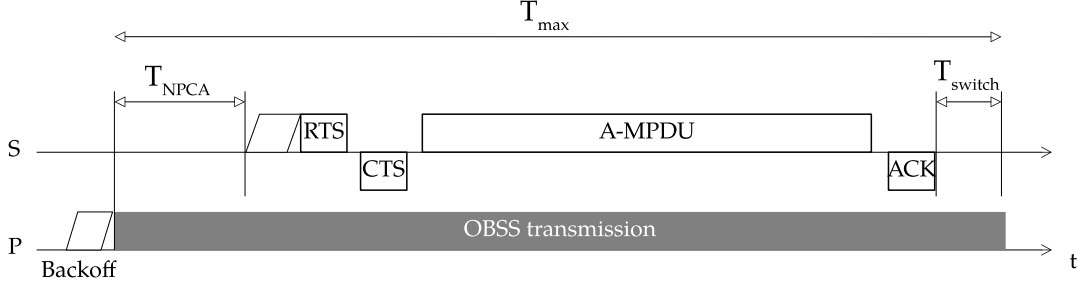


Fig. 2: Non Primary Channel Access operation.

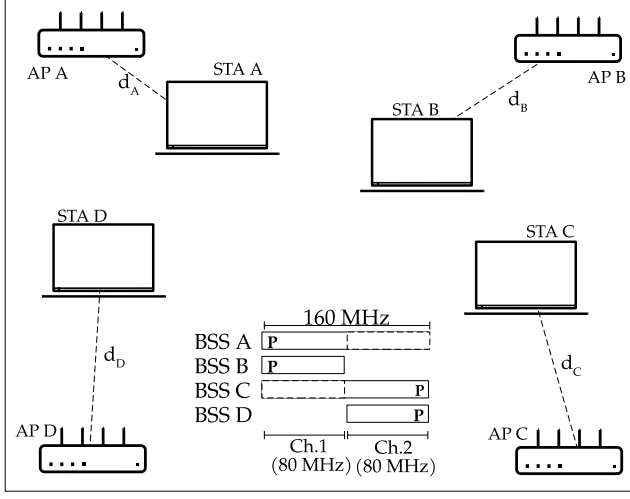


Fig. 3: Four overlapping BSSs.

packet has a size of L bits. A-MPDU packet aggregation is employed, with N packets aggregated per transmission. The value of N depends on the MCS, channel width, the maximum TXOP duration T_{\max} , and the maximum A-MPDU size Δ . Specifically, $N \leq \min(M, \Delta)$, where M is the maximum number of packets that can be transmitted within T_{\max} for a given MCS and channel width. For example, using MCS 11, BSS A can transmit up to 485 data packets of 1400 bytes each (approximately 5.4 Mbits) within T_{\max} on a 160 MHz channel. In contrast, with MCS 1 on an 80 MHz channel, BSS A can transmit up to 13 packets (approximately 145 kbits) during the same duration.

IV. MODELING NPCA WITH CTMCs

CTMC models are widely adopted for their ability to effectively capture the complex, asynchronous interactions among devices sharing spectrum resources through CSMA/CA, as in Wi-Fi networks. These models have been validated against simulations in [6], [8]–[11], [13], [14], demonstrating their accuracy, representativeness, and consistency.

A CTMC model captures the system's dynamics, enabling the analysis of its steady-state performance [5]. In applying CTMCs to characterize Wi-Fi, we consider that a state $s \in \otimes$ —where \otimes is the set of all CTMC states—is defined as the set of active BSSs (i.e., BSSs that are concurrently transmitting), and we assume that channel access contention and

transmission durations are governed by stochastic processes that follow exponential distributions.

However, CTMCs cannot accurately model collisions between contending devices. Specifically, because channel access times are exponentially distributed, two devices will never access the channel simultaneously, and therefore, collisions are effectively excluded. In our scenario, the impact of neglecting collisions is minimal because the number of contenders is small—resulting in a low collision probability by default—and also the use of RTS/CTS minimizes the duration of collisions. Consequently, neglecting collisions does not significantly affect the overall system performance. Nonetheless, the impact of collisions can be incorporated in CTMCs-based models using the approach outlined in [13].

The stationary distribution ($\bar{\pi}$) of a CTMC is derived by solving $\bar{\pi}\mathbf{Q} = 0$, where \mathbf{Q} is the infinitesimal generator matrix of the stochastic process. Each element of \mathbf{Q} , denoted $Q_{i,j}$, represents the transition rate from state i to state j . Forward transitions (e.g., initiating a transmission) occur at rate λ , while backward transitions (e.g., completing a transmission) occur at rate μ .

A. CTMC States

To model our described scenario, which includes NPCA transmissions, we adopt the approach used in [9], [10] for analyzing Dynamic Channel Bonding (DCB). However, in this paper we introduce a new type of state, referred to as NPCA state, representing the system state where NPCA transmissions occur. NPCA states become feasible when a BSS supporting NPCA detects that its primary channel is occupied by a transmission from an OBSS. If the secondary channel of the NPCA-enabled BSS is available, it then initiates (after contending) a transmission on that channel, adhering to the NPCA operation outlined in Section II. A key characteristic of NPCA states is that once the OBSS transmission completes, the system transitions to the same backward state that results from the end of the OBSS transmission.

Fig. 4 illustrates the CTMC for the Wi-Fi deployment depicted in Fig. 3, comparing two scenarios: (a) when NPCA is not supported (or disabled), and (b) when NPCA is enabled. Each state is identified by the BSSs transmitting simultaneously (the capital letters), along with the specific channels each one uses (indicated by subscripts). For example, state A_{12} denotes BSS A transmitting alone over Ch#1 and 2 (a 160 MHz transmission), while state B_1D_2 indicates that BSS

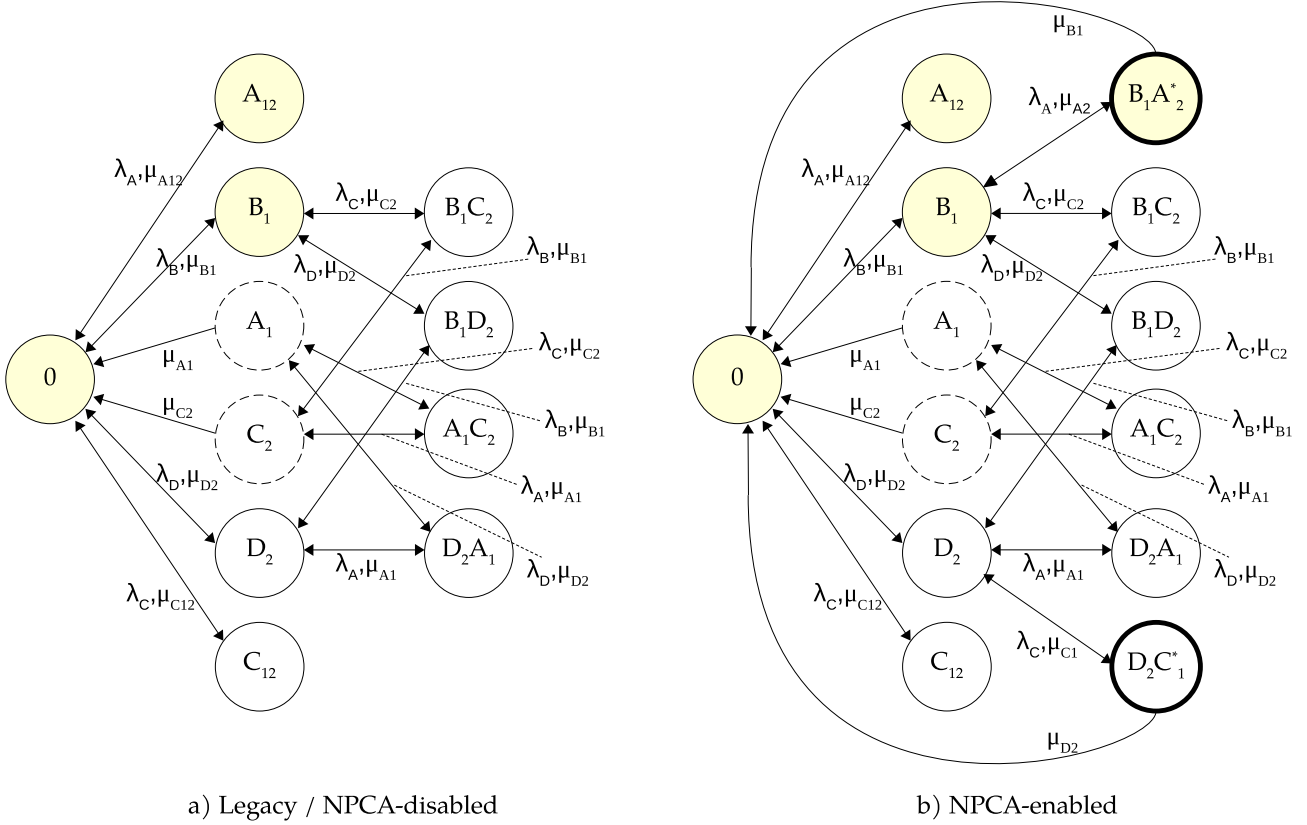


Fig. 4: CTMC modeling the Wi-Fi deployment shown in Fig. 3 when a) NPCA disabled, and b) NPCA is enabled.

B and BSS D are transmitting concurrently—BSS B using Ch#1 and BSS D using Ch#2, each performing 80 MHz transmissions. States outlined with dashed lines correspond to Dynamic Channel Bonding (DCB) operations. As detailed in [9], [10], these states arise when a BSS transmits over only a portion of its allocated channel. DCB states cannot be reached from the idle state (state 0), since a BSS will not voluntarily access just a fraction of its allocated bandwidth when the entire channel is available. States in which only BSSs A and B are active are highlighted in yellow, corresponding to the active states of Scenario I described in Section V. Without NPCA (Fig. 4.a), when BSS B (or BSS D) accesses Ch#1 (or Ch#2), the other channel can only be used by BSSs C and D (or BSSs A and B, respectively). For instance, from state B_1 , the system can only transition to states B_1C_2 or B_1D_2 . When NPCA is enabled (Fig. 4.b), two additional states become available: $B_1A_2^*$ and $D_2C_1^*$. These states represent scenarios where BSS A or BSS C initiates a transmission on their NPCA channel while their respective primary channel is occupied by BSS B or BSS D. Transitions from these NPCA states return to state 0 upon the completion of the OBSS transmission that initially blocked access on the primary channel. As explained in Section II, during this interval, multiple consecutive NPCA transmissions may occur if the NPCA-enabled BSS (e.g., BSS A) completes its transmission quickly but still has packets queued in its buffer.

The CTMC states reveal that enabling NPCA increases contention, as illustrated in Fig. 4b with the higher number

of forward transitions from states B_1 and D_2 compared to the same states in Fig. 4a, which entail that a bigger set of contenders is competing for the channel. The additional contention introduced by NPCA can be mitigated by configuring NPCA transmissions to use more conservative backoff parameters, such as a larger contention window (CW). However, this question lies beyond the scope of this paper.

B. CTMC Transitions

1) *Channel access rate, λ* : The transmission attempt rate, i.e., how aggressively a device contends to access the channel, is defined as the reciprocal of the expected backoff time, given by

$$\lambda = \frac{1}{E[\text{backoff}]} = \frac{2}{(CW - 1)T_e}, \quad (1)$$

where T_e is the duration of an empty slot (9 μ s).

2) *Transmission rate, μ* : The mean transmission duration $\mathbb{E}[T_s] = 1/\mu$ represents the time a device occupies the channel after gaining access. We follow the frames and intervals specified by the IEEE 802.11 protocol. In particular, the duration of an A-MPDU transmission comprising N packets is given by:

$$T_s = T_{\text{RTS}} + 3 \cdot T_{\text{SIFS}} + T_{\text{CTS}} + T_{\text{DATA}} + T_{\text{ACK}} + T_{\text{DIFS}} + T_e, \quad (2)$$

where

$$T_{\text{DATA}} = T_{\text{PHY}} + \left\lceil \frac{L_H + N(L_D + L) + L_T}{\text{DBPS}} \right\rceil T_{\text{OFDM}}, \quad (3)$$

with L_H as the MAC header, L_D as the MPDU delimiter, L as the MPDU size, and L_T as the tail bits. DBPS denotes the data bits per symbol, which depends on the number of subcarriers (and therefore of the channel width), the number of spatial streams, and the MCS used.

For NPCA transmissions, the maximum transmission duration is determined by the OBSS transmission duration, i.e., $T_{s,OBSS}$, and includes additional overheads: the time required to switch to the NPCA primary channel (T_{NPCA}) and to return to the original primary channel (T_{switch}). Consequently, the effective transmission time for NPCA is $T_{s,OBSS} - T_{NPCA} - T_{switch}$.

In both legacy (i.e., NPCA disabled) and NPCA transmissions, the number of packets transmitted is calculated as the maximum number of packets that can be aggregated within the available time, limited by the maximum A-MPDU size (Δ) as described in Section IV.

C. Performance Metrics

In this paper, we consider two performance metrics as described next.

Throughput (bps): The throughput $\Gamma^{(n)}$ of BSS n is defined as

$$\Gamma_n = \sum_{\forall s \in \Omega: n \in s} \pi_s (\mu_n^s N_n^s L), \quad (4)$$

where $\mu_n^s N_n^s L$ is the amount of data bits/second effectively transmitted when the system is in state s by BSS n .

Channel access delay (ms): To estimate the channel access delay, we perform an event-based simulation based on the \mathbf{Q} matrix. Given the current state, we identify the event that will happen first and transition to the corresponding next state, updating the system time. Throughout the simulation, we record the time intervals between consecutive transmissions for each BSS. These intervals reflect both the probability of successfully accessing the channel and the time spent deferring due to contention, and include the total time a BSS defers and transmits. All simulations start at state 0.

V. PERFORMANCE EVALUATION

A. Scenarios

We study the performance evaluation of NPCA in three representative scenarios that are extracted from the deployment of Fig. 3. These three scenarios cover the most important aspects needed to study NPCA performance. Considering more BSSs will only increase contention, proportionally scaling the performance each BSS can achieve, without providing further insights. Results in other scenarios can easily be extrapolated from the ones presented in this paper.

- 1) **Scenario I:** BSSs A and B are active. This scenario provides the most favorable conditions to evaluate NPCA throughput gains for BSS A, as its secondary 80 MHz channel remains always available. NPCA is expected to increase BSS A's channel access rate, enhancing throughput and reducing access delay.
- 2) **Scenario II:** BSSs A, B, and D are active. Compared to Scenario I, activating BSS D occupies BSS A's secondary 80 MHz channel, limiting NPCA transmission

Parameter	Value	Parameter	Value
CW_{min}	16	L	1400 Bytes
d	[1-17] meters	MCSs (11ax)	[1-11]
T_{max}	5 ms	Num SS.	2
Δ	[1-1024]	PER	0.1
T_{NPCA}	0.136 ms	T_{switch}	16 μs
OFDM symbol (std GI)	13.6 μs	Backoff slot	9 μs
DIFS	34 μs	SIFS	16 μs
Leg. PHY pream.	20 μs	PHY pream.	100 μs
RTS	160 bits	CTS	112 bits
MAC header	240 bits	BACK	240 bits
MPDU Del.	32 bits	Tail Bits	18 bits

TABLE I: Value of the parameters used in the performance evaluation.

opportunities. This scenario examines how activity on BSS A's secondary channel impacts NPCA gains.

- 3) **Scenario III:** All four BSSs are active. This creates a symmetric scenario where BSS A and BSS C utilize NPCA to access channels 2 and 1, respectively. We investigate whether NPCA still provides performance gains in such a balanced setting.

In Table I we show the parameters used in the performance evaluation. All the other non-specified parameters follow IEEE 802.11 specifications. If different values are considered during the evaluation, this will be indicated where it corresponds. For each point in the results, 5000 random instances of a given scenario have been simulated, which each instance lasting 500 s.

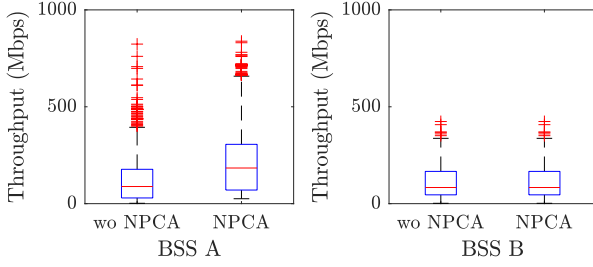
B. NPCA Throughput and Channel Access Delay Gains

We study the NPCA throughput and delay gains in Scenario I, where the secondary 80 MHz channel of BSS A—its NPCA channel—is always available. In this scenario, when NPCA is enabled, BSS A is able to access its secondary channel (Ch#2) when its primary channel (Ch#1) is busy, hence obtaining both higher throughput and lower channel access delay.

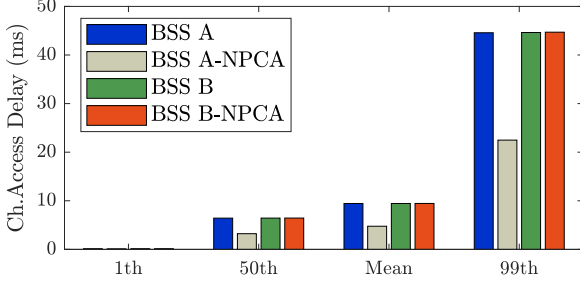
Throughput and channel access delay distributions are derived from multiple scenario instances. In each instance, we randomize two parameters per BSS: *i)* the station positions, placing them around their corresponding AP at distances between 1 and 17 meters, with MCSs assigned accordingly, and *ii)* the maximum A-MPDU value (Δ), ranging from 1 to its upper limit (1024), to introduce high variability in transmission durations. For reference, in Scenario I, when BSS A uses MCS 11 (1024-QAM, coding rate 3/4) over a 160 MHz channel, it can transmit A-MPDUs of up to 485 packets (each 1400 bytes) within a single TXOP, constrained by the maximum TXOP duration ($T_{max} = 5$ ms). Similarly, both BSSs A and B, operating with MCS 11 on an 80 MHz channel, can transmit up to 281 packets per TXOP.

Fig. 5a shows the throughput distribution as a boxplot¹ for BSSs A and B without and with NPCA enabled. Without NPCA, since BSS A and BSS B share the same primary channel and use the same CW_{min} , following CSMA/CA

¹A boxplot shows the median (line inside the box), the worst/best performance quartiles, i.e., 25%-iles (top and bottom edges of the box, respectively), and the maximum/minimum values (whisker lines outside the box).



(a) Throughput distribution.

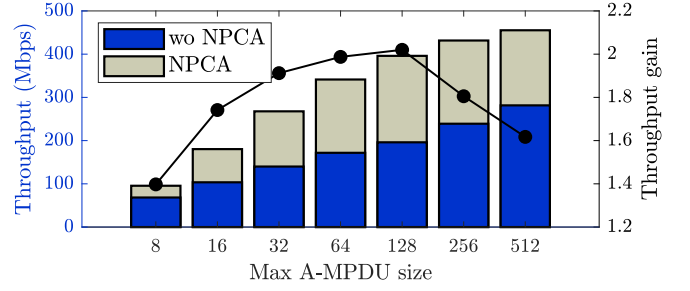


(b) Channel Access Delay percentiles.

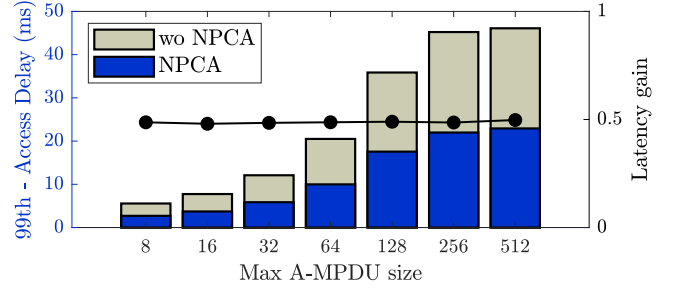
Fig. 5: Throughput and channel access delay results obtained in Scenario I.

operation they access the channel the same number of times on average. Therefore, the higher throughput achieved by BSS A is only because it is able to transmit using the full 160 MHz channel every time it accesses the channel, which turns out on more packets transmitted per TXOP. Enabling NPCA increases the throughput of BSS A, as it now can access its secondary 80 MHz channel (Ch#2) when BSS B is occupying its primary 80 MHz channel (Ch#1) while before it had to defer. In detail, enabling NPCA, the 75th percentile of BSS A's throughput increases by a factor of 1.73, the median by a factor of 2, and the 25th percentile by a factor of 2.41. This is an interesting result as it shows that NPCA gains are higher at the low percentiles, which can be seen as improving the throughput reliability of the network. As expected, BSS B is not affected by BSS A's NPCA transmissions—which happen at the same time but on a different channel—and hence, its throughput distribution remains exactly the same.

Throughput gains come from more frequent channel accesses, and therefore a proportional reduction on the channel access delay should be also expected. Fig. 5b shows different percentiles of the delay between two consecutive channel accesses by each BSS. With NPCA enabled, BSS A 99th and 50th channel access delay percentiles reduce, respectively, from 44.6 ms to 22.5 ms, and from 6.42 ms to 3.22 ms, which roughly represents a 50% reduction. These results confirm BSS A is able to access the channel almost twice as fast with NPCA than without it. As before, the channel access delay from BSS B is not affected when NPCA is enabled. Fig. 5b also includes the mean channel access delay, which for BSS A is 9.47 ms without NPCA, and 4.57 ms with NPCA. Without NPCA, on average BSS A will alternate transmissions with BSS B, and so it will access the channel approximately every



(a) Mean Throughput.



(b) Channel Access Delay.

Fig. 6: Throughput and channel access delay in BSS A for different maximum A-MPDU (Δ) values in Scenario I.

10 ms (i.e., the first 5 ms account for its own transmission, and the second 5 ms account for the transmission of BSS B). With NPCA, BSS A can always seize a TXOP and transmit, either on Ch#1 or in Ch#1-2, which justifies the observed channel access delay.

Highlight: NPCA improves throughput and reliability by enabling access to secondary channels when the primary is occupied. Overlapping OBSS transmissions—occupying only the NPCA channel of the NPCA-enabled BSS—remain unaffected, as NPCA operates on different channels, ensuring no negative impact on them. Channel access delay is nearly halved, enabling faster and more frequent transmissions.

C. A-MPDU Size for Maximum NPCA Gain

NPCA transmissions benefit from longer OBSS transmissions. Here, considering Scenario I, we investigate how different A-MPDU sizes affect the NPCA throughput and channel access delay gains. To do so, we test different maximum A-MPDU values (Δ). Therefore, now, all transmissions include $\min(M, \Delta)$ packets, where M is the maximum number of packets that can be included in a $T_{\max} = 5$ ms transmission, and depend on the employed MCS and channel width. Distance between each AP and its station is randomly selected in each scenario instance between 1 m and 17 m, as in the previous section.

Fig. 6a shows the mean throughput for BSS A with NPCA disabled (blue) and enabled (beige). The NPCA gain, defined as the ratio between the throughput with and without NPCA, increases with Δ due to longer OBSS transmissions by BSS B, which in turn allow for longer NPCA transmissions. The

maximum gain is observed at a maximum A-MPDU size of $\Delta = 128$ packets. One may wonder why the gain decreases afterward, despite the throughput continuing to rise until it saturates at $\Delta = 512$ packets. The reason lies in the transmission duration constraint: BSS B's transmissions are already limited by the maximum TXOP duration (5 ms). Consequently, although BSS A can include more packets in its 160 MHz transmissions, the throughput of BSS A's NPCA transmissions on Ch#2 (80 MHz) is also limited by the maximum TXOP duration. The observed throughput gains beyond this point come solely from the 160 MHz transmissions.

Regarding the 99th percentile of BSS A's channel access delay (Fig. 6b), it increases with the maximum A-MPDU size due to longer transmission durations. Interestingly, the ratio between the baseline and NPCA delay remains constant across all A-MPDU sizes, approximately equal to 0.5. Although not shown, this trend holds for other percentiles as well.

As for BSS B, although not shown, its behavior follows the pattern described in the previous section. Increasing the maximum A-MPDU size leads to higher throughput and channel access delay. When the A-MPDU size is small enough for BSS B to transmit all packets within the TXOP, it achieves the same throughput as BSS A without NPCA. However, once it becomes unable to fit as many packets per TXOP, its throughput falls slightly below that of BSS A without NPCA.

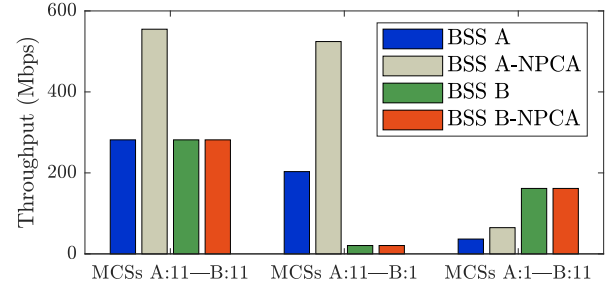
Highlight: The NPCA throughput gain is limited by the duration of OBSS transmissions and is therefore influenced by the A-MPDU size. Meanwhile, the channel access delay with NPCA remains consistently half that of the baseline across all A-MPDU sizes, as NPCA enables near-continuous transmissions.

D. Overcoming the OBSS Performance Anomaly

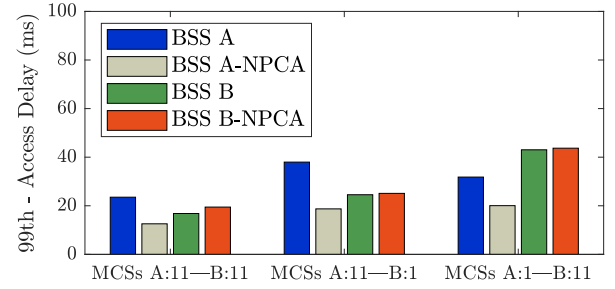
In the previous subsections, we analyzed multiple instances of Scenario I, where stations were randomly deployed within the coverage area, resulting in diverse MCSs. Here, we focus on specific cases where BSS A and B use either the lowest MCS (MCS 1, BPSK 1/2) or the highest MCS (MCS 11, 1024-QAM 3/4), with a maximum A-MPDU size of 128 packets. Our primary objective is to assess whether NPCA can mitigate the OBSS 802.11 performance anomaly—a phenomenon where long OBSS transmissions due to a low MCS degrade the throughput of all OBSSs, including those using higher MCS values. This effect was first described in [15] for a single, multi-rate BSS.

Fig. 7a presents the mean throughput for BSS A and B, with and without NPCA, across three MCS combinations:

- 1) *Both BSSs using MCS 11:* Without NPCA, BSS A and B achieve equal throughput (281 Mbps) as both transmit 128 packets per channel access. With NPCA, BSS A leverages its secondary 80 MHz channel (i.e., the NPCA primary channel) during BSS B's transmissions, increasing its throughput to 554 Mbps ($\times 1.9$ gain). As expected, BSS B's throughput remains the same.
- 2) *BSS A using MCS 11, BSS B using MCS 1:* Without NPCA, BSS A's throughput drops from 281 to 203 Mbps



(a) Mean Throughput.



(b) Channel Access Delay.

Fig. 7: Throughput and channel access delay when BSS A and B use different MCSs, without and with NPCA, in Scenario I.

because BSS B's transmission duration increases from 2.93 ms to 5 ms, reducing BSS A's channel access rate. BSS B, despite its prolonged transmission time, delivers only 13 packets, achieving a low throughput of 20 Mbps. With NPCA, BSS A exploits BSS B's extended transmission periods to send more than 128 packets across multiple consecutive NPCA transmissions. Specifically, after completing an NPCA transmission with 128 packets (the A-MPDU limit), BSS A, recognizing that its primary channel is still occupied by BSS B, initiates additional NPCA transmissions as described in Section II. This process repeats until the NPCA opportunity ends, boosting BSS A's throughput to 504 Mbps ($\times 2.5$ gain). These results highlight NPCA's effectiveness in mitigating the negative impact of long OBSS transmissions.

- 3) *BSS A using MCS 1, BSS B using MCS 11:* Without NPCA, the roles reverse, with BSS A experiencing limited throughput due to its low MCS, penalizing also BSS B. Enabling NPCA provides moderate gains, as BSS A's low MCS and BSS B's shorter transmissions limit the extent of improvement. However, BSS A still achieves a $\times 1.77$ throughput gain, which, while lower than in previous cases, remains significant.

Fig. 7b further illustrates the 99th-percentile delay. When one OBSS operates at a high MCS, it reduces the channel access delay for the other, and vice versa. These results align with the throughput analysis, reinforcing NPCA's effectiveness in addressing the OBSS performance anomaly.

Highlight: NPCA effectively mitigates the OBSS performance anomaly. When one OBSS operates at a low MCS, prolonged

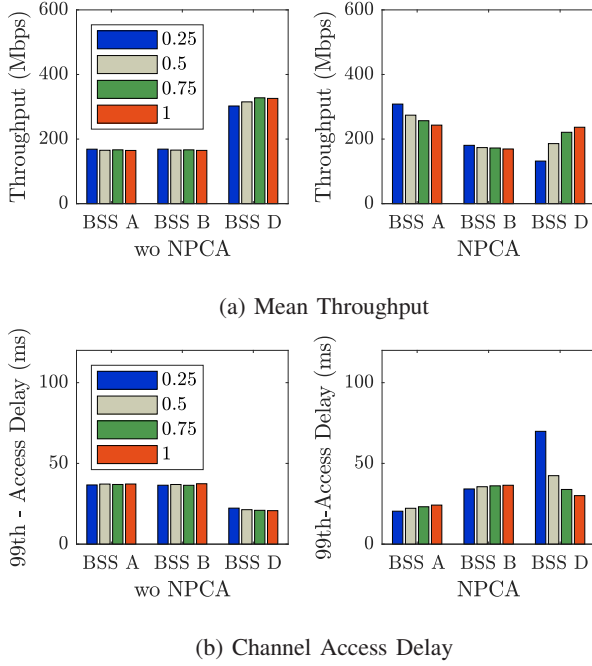


Fig. 8: Mean throughput and channel access delay for BSSs A, B and D in Scenario II.

transmissions degrade the overall network throughput. NPCA allows high-MCS BSSs to leverage these extended NPCA opportunities, significantly improving throughput.

E. Secondary Channel Activity: A Zero-sum Game?

In this section, we investigate the impact of OBSS activity on BSS A's NPCA channel (Ch#2) in terms of achievable throughput, considering *Scenario II*, where BSSs A, B, and D are active. Specifically, we examine the effect of varying BSS D's activity levels. To model this, we adjust BSS D's contention aggressiveness by scaling its channel access rate λ with the parameter α_D , thereby controlling its channel access intensity (i.e., high (low) values of α_D correspond to low (high) backoff values). We assume a maximum A-MPDU size of $\Delta = 128$ packets and randomize station positions by placing them around their respective APs at distances between 1 and 17 meters.

In this Scenario II, when NPCA is not enabled, the asynchronous operation among the BSSs significantly limits BSS A's ability to utilize the full 160 MHz bandwidth. Even at low values of α_D , Ch#2 is almost continuously occupied by BSS D, forcing BSS A to transmit only on Ch#1. In this configuration, BSSs A and B typically alternate access to Ch#1, while Ch#2 remains exclusively used by BSS D. However, when NPCA is enabled, BSS A gains additional opportunities to contend with BSS D. While BSS B occupies Ch#1, BSS A switches to its NPCA channel (Ch#2) and attempt to access the medium there, contending with BSS D as mentioned.

Fig. 8a (left side) illustrates the mean throughput of BSSs A, B, and D when NPCA is not enabled. In this scenario, increasing α_D has an almost negligible effect overall. For BSSs A

and B, increasing α_D slightly decreases their throughput, as it reduces the likelihood of 160 MHz transmissions by BSS A. For BSS D, a higher α_D reduces its contention time for channel access, thereby also decreasing BSS A's transmission opportunities on Ch#2, and resulting in higher throughput for BSS D.

The mean throughput of each BSS when NPCA is enabled is shown in Fig. 8a (right side). As discussed earlier, NPCA allows BSS A to directly contend with BSS D for access to Ch#2 when Ch#1 is occupied by BSS B. This ability to compete in both channels increases BSS A's transmission opportunities compared to BSS B and D, resulting in higher throughput for BSS A. Furthermore, since BSS A and BSS D now compete for the access to Ch#2, the impact of α_D on BSS A's throughput becomes significant. For low values of α_D (i.e., large backoff intervals for BSS D), BSS A has more chances of accessing Ch#2, as reflected in the figure. Overall, increasing α_D shifts throughput from BSS A to BSS D, with both achieving comparable performance when $\alpha_D = 1$. Finally, as expected, BSS B's throughput remains unaffected by changes in BSS D's activity.

When comparing the aggregate throughput—sum of the individual throughput of BSSs A, B and D—with and without NPCA, the difference is minimal. For instance, at $\alpha_D = 1$, the aggregate throughput without NPCA is 655 Mbps, which decreases to 649 Mbps with NPCA. With NPCA, two factors contribute to the slight throughput loss: *i*) increased contention between BSS A and D on Ch#2, and *ii*) the additional transmission overhead introduced by NPCA. Thus, while NPCA does not significantly affect the aggregate throughput, it affects how the throughput is shared among the BSSs.

Fig. 8b presents the 99th-percentile channel access delay. The delay trends mirror the throughput results, illustrating how enabling NPCA benefits BSS A at the expense of BSS D. Notably, for low α_D values, BSS D experiences higher delays due to extended backoff periods.

Highlight: With NPCA enabled, BSSs A and D contend for access to Ch#2, making their throughputs and channel access delays mutually sensitive to each other's activity levels. Although NPCA introduces additional contention and overhead, its impact on aggregate throughput remains minimal. Nevertheless, while it represents a zero-sum game in terms of aggregate throughput, NPCA significantly reshapes the utilization of spectrum resources. This underscores the importance of accounting for NPCA in future Wi-Fi channel allocation strategies.

F. Multiple NPCA BSSs Contending

Finally, we consider Scenario III, where BSS C is activated to analyze a setup in which two BSSs—namely BSS A and BSS C—support NPCA transmissions. In this scenario, BSS C performs NPCA transmissions on Ch#1 (its NPCA channel) when its primary channel, Ch#2, is occupied by BSS D. As in the previous section, we vary the activity factor of BSS D from $\alpha_D = 0.25$ to 1. Stations are uniformly distributed between 1 and 17 meters from their respective APs, and the maximum

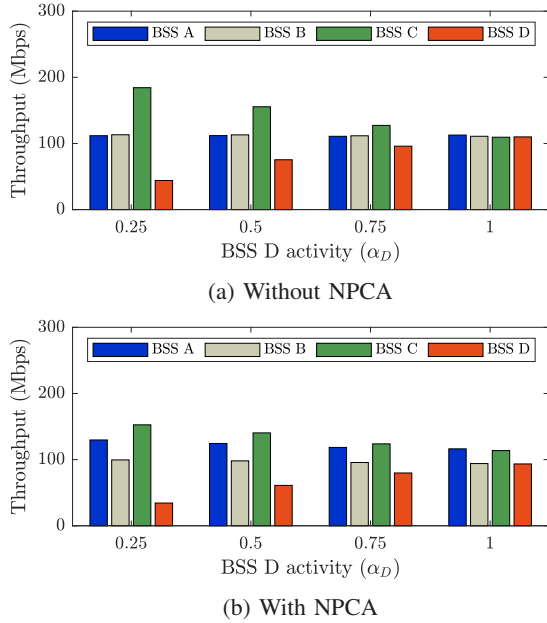


Fig. 9: Mean throughput (Mbps) for each BSS without and with NPCA in Scenario III.

A-MPDU size is set to $\Delta = 128$ packets. Note that we do not present channel access delay results for this scenario, as they do not provide additional insights.

Fig. 9b shows the throughput for each BSS, both without and with NPCA enabled, as the activity factor of BSS D increases. Without NPCA, increasing α_D leads to reduced throughput for BSS C due to increased contention with BSS D on Ch#2. BSS A and B remain unaffected. At $\alpha_D = 1$, the symmetry of the scenario ensures that all four BSSs achieve the same throughput. With NPCA enabled, BSS A and BSS C can now transmit using NPCA on Ch#2 and Ch#1, respectively, which makes them to interact. We observe the following: *i*) for $\alpha_D < 1$, BSS A benefits from more NPCA transmission opportunities than BSS C because BSS B is more active than BSS D. This results in a significant throughput gain for BSS A, at the expense of BSS C. For instance, at $\alpha_D = 0.25$, BSS A's throughput increases from 111 Mbps to 129 Mbps (a 16% gain), while BSS C's throughput drops from 184 Mbps to 152 Mbps (a 17% loss). As α_D approaches 1, the throughput of BSS A and C equalizes; *ii*) BSS B's throughput decreases with NPCA enabled, since BSS C now competes for Ch#1. This degradation becomes more pronounced as BSS D's activity increases, allowing more frequent NPCA transmissions by BSS C on Ch#1; *iii*) For $\alpha_D < 1$, as discussed before, BSS C sees reduced throughput under NPCA due to BSS A benefiting more from NPCA opportunities on Ch#2, driven by BSS B's higher activity compared to BSS D; and, *iv*) BSS D's throughput increases with α_D and mirrors the behavior of BSS B when $\alpha_D = 1$.

Highlight: While OBSS transmissions on a NPCA-enabled BSS's primary channel may allow it to benefit from additional transmissions on its secondary channel, it is generally

preferable—in terms of achievable throughput—to avoid such OBSS activity whenever possible. In symmetric scenarios where avoidance is not feasible, NPCA can still provide a throughput gain, albeit at the expense of non-NPCA BSSs, due to increased contention on their channels.

VI. RELATED WORK

NPCA was introduced in the 802.11 Ultra High Reliability (UHR) Study Group (SG) as a potential feature for Wi-Fi 8, outlining its basic operation for both APs and stations [16]. Illustrative results (simulation only) to demonstrate potential performance gains were also presented in the UHR SG [17], [18]. Specifically, [17] provided throughput results for scenarios involving two BSSs (1 OBSS) and three BSSs (2 OBSSs), corresponding to our Scenarios I and II. Similarly, [18] reported simulation results for a scenario akin to our Scenario II, considering both full-buffer and finite-load traffic, along with latency measurements. In both works, the results align with the findings in this paper, showing similar improvements in throughput and latency.

The discussion on NPCA continued in the 802.11bn Task Group (TGbn), with a focus on implementation details. Key on-going considerations include the conditions that should trigger a switch when the primary channel is busy [19], challenges in detecting OBSS transmissions and their bandwidth when not all devices in the NPCA BSS observe them [20], and the configuration of EDCA parameters (e.g., parameter sets, reuse of backoff counters) and wide-bandwidth transmissions for NPCA [21].

Outside the 802.11 community, research on NPCA is limited, with the exception of [22], which presents an analytical model of NPCA based on Bianchi's model [23]. Unlike our analysis, the model in [22] assumes that all BSSs share the same primary channel (i.e., Scenario I) and does not cover Scenarios II and III. Instead, its focus is on the impact of increasing the number of stations and including uplink transmissions. Nonetheless, the conclusions in [22] regarding throughput and latency gains are consistent with ours.

In summary, we advance beyond the state of the art by presenting a comprehensive analysis capable of capturing complex scenarios involving multiple BSSs. Our results account for various critical aspects of Wi-Fi, including the effects of different MCSs and TXOP durations. Furthermore, we highlight the OBSS performance anomaly, demonstrating how NPCA effectively mitigates its negative effects on performance. Additionally, we provide insights into how NPCA can increase contention in high-traffic scenarios, offering a detailed understanding of its trade-offs and potential in future Wi-Fi deployments.

VII. CONCLUSIONS

In this paper, we have studied the Non-Primary Channel Access mechanism, a distinctive feature envisioned for future IEEE 802.11bn Wi-Fi networks. NPCA enables devices to contend and transmit on a secondary channel when the primary channel is occupied by a transmission from an Overlapping Basic Service Set, thereby reducing channel access delay

and improving throughput. Notably, NPCA proves particularly effective in mitigating the OBSS performance anomaly, as low-rate, long-duration transmissions create opportunities for similarly long NPCA transmissions. However, as expected, enabling NPCA also increases contention on secondary channels, potentially degrading performance for BSSs operating on those channels.

To analyze NPCA operation, we developed a Continuous-Time Markov Chain modeling approach, which offers a valuable framework to characterize the interactions among overlapping BSSs when NPCA is enabled. While remaining tractable, the model provides unique and valuable insights into the potential benefits and limitations of NPCA in dense WLANs.

Several open research questions remain. For example, future work could investigate NPCA's performance under mixed traffic conditions, where NPCA opportunities are only leveraged by low-latency traffic. This approach could leverage NPCA's reduced channel access delay while minimizing contention with neighboring networks operating on the secondary channel. Moreover, the concept of channel switching could be further generalized by enabling NPCA transmissions to opportunistically utilize any available idle channel, rather than being limited to use the secondary one. This would increase the chances of successful transmissions and further reduce OBSS contention.

ACKNOWLEDGMENTS

B. Bellalta and F. Wilhelmi were in part supported by grant Wi-XR PID2021-123995NB-I00 (MCIU/AEI/FEDER,UE), MdM CEX2021-001195-M (MCIU/AEI/10.13039/501100011033), and by SGR 00955-2021 AGAUR. L. Galati Giordano was in part supported by UNITY-6G project, funded from European Union's Horizon Europe Smart Networks and Services Joint Undertaking (SNS JU) research and innovation programme under the Grant Agreement No 101192650. G. Geraci was in part supported by the Spanish Research Agency through grants PID2021-123999OB-I00, CEX2021-001195-M, and CNS2023-145384. We have used ChatGPT for editing and grammar enhancements.

REFERENCES

- [1] S. Barrachina-Muñoz, B. Bellalta, and E. W. Knightly, "Wi-Fi channel bonding: An all-channel system and experimental study from urban hotspots to a sold-out stadium," *IEEE/ACM Transactions on Networking*, vol. 29, no. 5, pp. 2101–2114, 2021.
- [2] E. Khorov, A. Kiryanov, A. Lyakhov, and G. Bianchi, "A tutorial on IEEE 802.11 ax high efficiency WLANs," *IEEE Communications Surveys & Tutorials*, vol. 21, no. 1, pp. 197–216, 2018.
- [3] L. Galati-Giordano, G. Geraci, M. Carrascosa, and B. Bellalta, "What will Wi-Fi 8 be? A primer on IEEE 802.11 bn ultra high reliability," *IEEE Communications Magazine*, vol. 62, no. 8, pp. 126–132, 2024.
- [4] I. Val, D. López-Pérez, A. Kijanka, S. Schelstraete, L. Muñoz, D. Arlandis, and M. Martínez, "Wi-Fi 8 unveiled: Key features, multi-AP coordination, and the role of C-TDMA," *techXriv*, 2025.
- [5] R. Boorstyn, A. Kershenbaum, B. Maglaris, and V. Sahin, "Throughput analysis in multihop CSMA packet radio networks," *IEEE Transactions on Communications*, vol. 35, no. 3, pp. 267–274, 1987.
- [6] S. C. Liew, C. H. Kai, H. C. Leung, and P. Wong, "Back-of-the-envelope computation of throughput distributions in CSMA wireless networks," *IEEE Transactions on Mobile Computing*, vol. 9, no. 9, pp. 1319–1331, 2010.

- [7] R. Laufer and L. Kleinrock, "The capacity of wireless CSMA/CA networks," *IEEE/ACM Transactions on Networking*, vol. 24, no. 3, pp. 1518–1532, 2015.
- [8] B. Bellalta, A. Checchio, A. Zocca, and J. Barcelo, "On the interactions between multiple overlapping WLANs using channel bonding," *IEEE Transactions on Vehicular Technology*, vol. 65, no. 2, pp. 796–812, 2015.
- [9] A. Faridi, B. Bellalta, and A. Checchio, "Analysis of dynamic channel bonding in dense networks of WLANs," *IEEE Transactions on Mobile Computing*, vol. 16, no. 8, pp. 2118–2131, 2016.
- [10] S. Barrachina-Munoz, F. Wilhelmi, and B. Bellalta, "Dynamic channel bonding in spatially distributed high-density WLANs," *IEEE Transactions on Mobile Computing*, vol. 19, no. 4, pp. 821–835, 2019.
- [11] F. Wilhelmi, S. Barrachina-Muñoz, C. Cano, I. Selinis, and B. Bellalta, "Spatial reuse in IEEE 802.11 ax WLANs," *Computer Communications*, vol. 170, pp. 65–83, 2021.
- [12] T. Adame, M. Carrascosa, and B. Bellalta, "The TMB path loss model for 5 GHz indoor WiFi scenarios: On the empirical relationship between RSSI, MCS, and spatial streams," in *2019 Wireless Days (WD)*. IEEE, 2019, pp. 1–8.
- [13] B. Bellalta, "Throughput analysis in high density WLANs," *IEEE Communications Letters*, vol. 21, no. 3, pp. 592–595, 2016.
- [14] S. Barrachina-Munoz, F. Wilhelmi, I. Selinis, and B. Bellalta, "Komondor: A wireless network simulator for next-generation high-density WLANs," in *2019 Wireless Days (WD)*. IEEE, 2019, pp. 1–8.
- [15] M. Heusse, F. Rousseau, G. Berger-Sabbatel, and A. Duda, "Performance anomaly of 802.11b," in *IEEE INFOCOM*, vol. 2. IEEE, 2003, pp. 836–843.
- [16] M. Park, et al., "Non-Primary Channel Access," IEEE 802.11-23/2005r1. 2023.
- [17] Y. Seok, et al., "Non-Primary Channel Access," IEEE 802.11-23/0797r1. 2023.
- [18] D. Dibakar, et al., "NPC sims follow-up," IEEE 802.11-23/1444r1. 2023.
- [19] V. Ratnam, et al., "Channel Switching Rules for NPCA," IEEE 802.11-24/1115r1. 2024.
- [20] S. Byeon, et al., "NPCA operation issue," IEEE 802.11-24/1394r0. 2024.
- [21] Donju Cha et al., "EDCA for Non Primary Channel Access," IEEE 802.11-24/0426r0. 2024.
- [22] D. Wei, L. Cao, L. Zhang, X. Gao, and H. Yin, "Non-primary channel access in IEEE 802.11 UHR: comprehensive analysis and evaluation," in *2024 IEEE 100th Vehicular Technology Conference (VTC2024-Fall)*. IEEE, 2024, pp. 1–6.
- [23] G. Bianchi, "Performance analysis of the IEEE 802.11 distributed coordination function," *IEEE Journal on Selected Areas in Communications*, vol. 18, no. 3, pp. 535–547, 2000.